

# Treatment Efficiency of UV/H<sub>2</sub>O<sub>2</sub> Process on Simulated Textile Industry Wastewater by using Box-Behnken Design (BBD) Coupled with Response Surface Methodology (RSM)

P. Sivakumar<sup>1</sup>, P. Sakthisharmila<sup>2</sup>

<sup>1,2</sup> Centre for Environmental Research, Department of Chemistry, Kongu Engineering College, Perundurai, Erode – 638052, TN, India

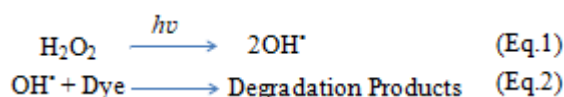
**Abstract:** The present study involves the performance evaluation of UV/H<sub>2</sub>O<sub>2</sub> process on a simulated dye bath effluent by studying the effects of initial H<sub>2</sub>O<sub>2</sub> concentration, changing the pollution load and initial pH. The process was optimized by four factors and three levels of Box-Behnken design (BBD) coupled with response surface methodology (RSM). During the experiment colour removal and degradation studies were also performed to ensure the treatment efficiency. The results obtained show that the colour removal efficiency can be achieved within a short time due to the degradation of the structure which is more susceptible to oxidation that undergoes faster degradation. Then slower and gradual degradation of the simple and conjugated aromatic compounds takes place. In the first 5 minutes of the irradiation of the dyes, the pH value is decreased from 11 to 9.5 and for another pH value decreased from 9 to 7.01. The drop in the pH value is mainly due to the formation of organic as well as inorganic acid as a degradation product. Under the optimum operating conditions such as pollution load of 64%, initial concentration of H<sub>2</sub>O<sub>2</sub> 0.6 M, initial pH value of 8 and treatment time of 81 min shows the predicted removal efficiencies are 98.77% and 86.11% for Colour removal and COD removal, respectively, which were closer to the experimental values are 98.11% and 85.26% for Colour removal and COD removal respectively.

**Keywords:** UV/H<sub>2</sub>O<sub>2</sub>, Box-Behnken design, color removal, COD, Effluent, degradation

## 1. Introduction

Dyeing and finishing process of the textile plants are produced high level of environmental contamination due to the high toxicity of the chemical components of the wastewater [1,2,3]. Azo dyes are the largest group of colourants to textile fabrics, which we mostly used for the production. These dyes contain one (mono azo), two (diazo) or more (polyazo) azo groups (-N=N-), which are linked to aromatic rings. Recently most of cellulosic fibers such as cotton and wool are dyed using reactive azo dyes. But such dyes possess low fixation rate and consumes more water for preparation, dyeing, washing and rinsing stages. Most of the unfixed dyes are discharged directly to the environment or after the partial treatment. Potentially carcinogenic aromatic amines may be produced by the metabolic cleavage of such complex dyes. Because of the complexity of the chemical structure, biological treatments are not efficient for the degradation.

The uses of conventional oxidants for the treatment of dye wastewater are not always feasible owing to thermodynamic and kinetic limitations of the common reagents [4,5,6]. Advanced oxidation processes (AOP) decompose the chromophore of the dye and consequently realize the complete decolourization. This can be possible by the generation of powerful hydroxyl radical with an oxidation potential of 2.80V which can oxidize broad range of organic compounds. A direct method for the generation of the hydroxyl radical is hydrogen peroxide photo cleavage by means of UV<sub>254</sub> radiation. [7,8,9,10,11].



The main objective of this investigation is to optimize the effect of UV/H<sub>2</sub>O<sub>2</sub> process on variable parameters such as initial pollution load, initial H<sub>2</sub>O<sub>2</sub> concentration and initial pH of the simulated wastewater on the colour removal and COD removal. The study also concentrates on the degradation of aromatic, azo and sulphonic functional groups in the dye. Finally the results were optimized using Box-Behnken experimental design with four factors and three levels of optimization for all the variables.

## 2. Materials and Methods

### 2.1 Simulated dye bath effluent

The exact composition of the simulated dye bath effluent is given in Table.1. The dyes used are of commercial grade and used throughout the experiments without further purification in order to represent the actual dyeing conditions. The other chemicals were of analytical grade and supplied by Merck. The dye bath effluent was simulated by dissolving proper amounts of three commercial dyes and dye assisting chemicals in hot deionized water (T = 70°C) which is a representative sample equivalent to the characteristics of real time effluent [12]. (Table 2).

**Table 1:** Composition of the Simulated dye bath effluent

S.No	Constituents	Concentration mg/L
1	Reactive Blue	600
2	Direct Red	600
3	Acid violet	600
4	Starch	500
5	Sucrose	500
6	NaCl	5000
7	Na <sub>2</sub> SO <sub>4</sub>	1000
8	Na <sub>2</sub> CO <sub>3</sub>	1000
9	NaHCO <sub>3</sub>	1000
10	Na <sub>2</sub> HPO <sub>4</sub>	500
11	NaOH	1200
12	Detergent	300

## 2.2 Photo reactor

Photoreactions were carried out in a glass photoreactor comprised of a quartz tube surrounded by a water cooling

jacket and immersed in a Pyrex cylinder. The working volume of the photoreactor is 150 ml. The 16 W low pressure mercury vapor lamp with maximum emission at 254 nm is used as a source of UV irradiation.

## 2.3 Experimental Procedure

Experiments were carried out with necessary quantity of the simulated dye bath effluent and H<sub>2</sub>O<sub>2</sub> into the photoreactor. The solution was magnetically stirred and the temperature was maintained at 25°C by circulation of water in the cooling jacket. The pH of the solution was measured by pH meter and adjusted by using dilute hydrochloric acid or sodium hydroxide. The samples were taken at definite time intervals to identify the loss of aromaticity of the dye during the photodegradation.

**Table 2:** Comparative physico-chemical characterization of simulated dye bath effluent with real time effluent<sup>12</sup>

Parameters	Typical characteristics of real time textile effluents					Simulated Dye bath Effluent
	Sruthi Dyeing, Veerapandi Pirivu, Tiruppur	CETP, Veerapandi, Tiruppur	CETP, Mannarai, Tiruppur	CETP, Mannarai, Tiruppur	Texwel Dyeing, SIDCO, Tiruppur	
pH	9.04	9.31	8.15	10.08	9.03	10.68
Conductivity (mScm-1)	8.13	8.64	8.88	14.79	10.78	19.4
COD (mg/l)	1580	780	1210	1460	1380	2794
TDS (mg/l)	8180	7100	6120	13000	7760	13630
Alkalinity (mg/l)	3225	1550	1475	7250	1675	2500
Total Hardness (mg/l)	4200	1280	3885	2590	1295	1315
Chloride (mg/l)	75	533	145	278	1668	5112
Sulfate (mg/l)	2496	2304	960	6300	2520	1750

## 2.4 Analytical Determination

The degradation of the effluent can be monitored by using UV visible spectrophotometer as a function of irradiation time at different wavelengths associated with simple aromatic (250 nm), aromatic carbonyl compounds (276 nm), conjugated dienes and/or polyaromatic (286 nm) and coloured compounds (523 nm). Decrease in Chemical Oxygen Demand (COD) and sulfur estimation were calculated to identify the mineralization rate. Standard analytical techniques were used as per the methods described by APHA, 2005 [13].

## 3. Result and Discussion

### 3.1 Effect of concentration of H<sub>2</sub>O<sub>2</sub>

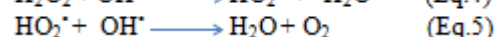
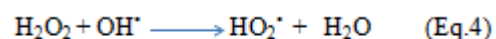
The experiments were carried out in the presence and absence of UV irradiation. Colour removal efficiency was less than 10% and no measurable removal efficiency was observed when it was carried out in UV and H<sub>2</sub>O<sub>2</sub> individually, which was in agreement with the literature [14]. Notable removal efficiency was observed when it was treated with the UV/H<sub>2</sub>O<sub>2</sub>, it can be explained by the fact that the formation of powerful oxidant, OH<sup>•</sup> radicals by direct photolysis of hydrogen peroxide (Eq. 1 & 2). Due to the low molar absorptivity of the hydrogen peroxide, theoretically excess of hydrogen peroxide is needed to produce more OH<sup>•</sup> radicals [15]. So the efficiency of the degradation of the simulated effluent depends mainly on the

concentration of the hydrogen peroxide. The concentration of hydrogen peroxide may either increase or decrease the degradation process. Therefore, it is essential to find out the optimum concentration of hydrogen peroxide for the better treatment efficiency. It was decided to conduct the experiment at the different initial concentration of hydrogen peroxide (0.1 to 1.0 M) and at fixed pollution load (60%) at pH 7 and at the temperature 25°C.

The first order rate equation (Eq.3) can be represented by the following differential rate law,

$$r = \frac{d[\text{simulated dye}]}{dt} = k[\text{Simulated dye}][\text{H}_2\text{O}_2] \quad (\text{Eq. 3})$$

The colour removal efficiency (Fig.1) was increased from 63.76 % to 98.77% with an increase of hydrogen peroxide concentration from 0.1 M to 0.4 M. Lower colour removal efficiency at 0.1 M is due to insufficient concentration of hydrogen peroxide for the generation of hydroxyl radicals. The quenching effect of hydrogen peroxide is observed at higher concentration of hydrogen peroxide (from 0.6 M to 1.0 M) leads to the lower colour removal efficiency (Eq.4 &5).



The correlation coefficient (R<sup>2</sup>) values explain the fitting extent of the functional equation and the experimental data (Table 3). Higher rate constant value (0.0295 min<sup>-1</sup>) at the concentration 0.4 M shows the optimized conditions for the effective colour removal efficiency of the process.

**Table 3:** First order rate constants for the decolourization of simulated dye at the pollution load 60% and at the pH 7 in the presence of UV light

S. No.	Concentration of H <sub>2</sub> O <sub>2</sub> (M)	R <sup>2</sup>	k (min <sup>-1</sup> )	Colour removal efficiency (%)
1	0.1	0.9115	0.0117	63.7602
2	0.2	0.9829	0.0186	93.6658
3	0.4	0.9616	0.0295	98.7705
4	0.6	0.9687	0.0280	98.6301
5	0.8	0.9762	0.0281	99.0728
6	1.0	0.9641	0.0300	98.6466

### 3.2 Effect of pollution load

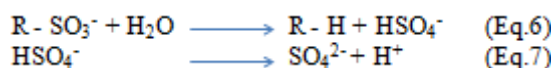
The effect of pollution load on the decolourization efficiency was monitored at different concentration level of pollution load and presented in Fig.2a. The colour removal efficiency was decreased with the increase of the pollution load from 20% to 100%. The molar absorption coefficient of the simulated dye at 254 nm is very high, so that an increase in the pollution load of the simulated dye effluent induces the internal optical density and the solution becomes highly impermeable to UV radiation. This may lead to the decrease in production of hydroxyl radicals and hence the removal efficiency is decreased.

**Table 4:** Variation of first order rate constants for the decolourization of simulated dye effluent with different pollution load and at 0.4 M initial H<sub>2</sub>O<sub>2</sub> concentration, at the pH 7 in the presence of UV light

Pollution Load (%)	Dye degradation kinetics					
	R <sup>2</sup> <sub>250 nm</sub>	k <sub>250 nm</sub> (min <sup>-1</sup> )	R <sup>2</sup> <sub>276 nm</sub>	k <sub>276 nm</sub> (min <sup>-1</sup> )	R <sup>2</sup> <sub>286 nm</sub>	k <sub>286 nm</sub> (min <sup>-1</sup> )
20	0.9398	0.0152	0.9685	0.0219	0.9667	0.0293
40	0.9649	0.0106	0.9679	0.0208	0.9733	0.0256
60	0.9847	0.0098	0.9773	0.0161	0.9849	0.0205
80	0.8213	0.0051	0.9705	0.0117	0.9544	0.0138
100	0.9097	0.0069	0.9910	0.0102	0.9924	0.0122

In association with colour removal efficiency, degradation kinetic behaviors were also analyzed for this condition to identify the extent of mineralization during the experiment. Table 4 shows the first order kinetics for the dye degradation at different UV range such as 250, 276 and 286 as a function of time to the simulated effluent during the irradiation process. It was observed that fast decolourization occurs in the first few minutes of irradiation, which indicates the beginning of degradation with the structure more susceptible to oxidation such as azo groups. Then slower and gradual degradation of the simple and conjugated aromatic compounds take place until they attain a complete mineralization. Decrease in the COD removal efficiency during the irradiation process will also support the slower rate of dye degradation (Fig.2b).

The formation of inorganic compounds lead to the formation of the sulfate ions, which is derived from organic sulfur (Eq.6 & 7). The only product expected from the sulfur containing dye is sulfate ion derived from the initial attack to the dye sulfonic groups [15].



At the beginning of the reaction high rate of sulfate ions are formed and then becomes stable, which confirms that dye sulfonic groups are attacked in the first few minutes of irradiation (Fig.3).

### 3.3 Effect of pH

Changes in the pH value of dye solutions as a function of the irradiation time for different initial pH values are shown in Fig.4a. Within first ten minutes of experiment initial pH value of the simulated dye bath effluent is decreased from 11 to 9.5 and from 9 to 7.01. The drop in the solution pH is mainly due to the formation of organic acid as well as inorganic acids during UV irradiation of simulated dye bath effluent. But in neutral (pH 7) and in acid medium (pH 3 & 5) the decrease of initial pH takes place only after 10 minutes of time. Significant drop in the solution pH by nearly 2.5 pH units are probably due to the formation of low molecular weight organic acid as a degradation product when the initial pH of the simulated dye bath effluent is at pH 5. On the other hand, in neutral medium (pH 7) and in acidic medium (pH 3), weak organic acids were formed as a degradation product and hence no significant changes were observed [16,17].

The influence of pH on the rate of decolourization of the simulated dye bath solution by UV/H<sub>2</sub>O<sub>2</sub> process was investigated at different pH values: 3.0, 5.0, 7.0, 9.0, and 11.0, using 60% pollution load solutions and 0.4 M H<sub>2</sub>O<sub>2</sub> (Fig. 4b). The colour removal efficiency was very less in acidic (pH 3), weak acidic (pH 5) and basic medium (pH 11) and it was more prominent in neutral (pH 7) and slightly basic medium (pH 9). The deactivation of OH<sup>•</sup> is more important when the pH of the solution is high. The reaction of OH<sup>•</sup> with HO<sub>2</sub><sup>-</sup> is approximately 300 times faster than its reaction with H<sub>2</sub>O<sub>2</sub>. The scavenging effect [18, 19] of inorganic anions present in the effluent (such as CO<sub>3</sub><sup>2-</sup>, SO<sub>4</sub><sup>2-</sup>, PO<sub>4</sub><sup>3-</sup>) decreased the colour removal efficiency of the radicals at the pH 3 and 5.

### 3.4 Optimization

Statistical experimental design was employed to determine the effects of operating variables on colour removal efficiency and to find the combination of variables resulting in maximum colour and COD removal efficiency. Three major steps in the optimization process involve; performing the statistically designed experiments, estimating the coefficients in a mathematical model and predicting the experimental outputs (as a response) and checking the suitability of the model. The minimum and maximum ranges for the four factors are illustrated in the Table 5. General form of a quadratic model for four variables is as given in Eq.8 [20, 21, 22 & 23].

$$Y = \beta_0 + \beta_1 X_1 + \beta_2 X_2 + \beta_3 X_3 + \beta_4 X_4 + \beta_{11} X_1^2 + \beta_{22} X_2^2 + \beta_{33} X_3^2 + \beta_{44} X_4^2 + \beta_{12} X_1 X_2 + \beta_{13} X_1 X_3 + \beta_{14} X_1 X_4 + \beta_{23} X_2 X_3 + \beta_{24} X_2 X_4 + \beta_{34} X_3 X_4 \quad \text{(Eq. 8)}$$

Where Y = predicted response,  $\beta_0$  = constant coefficient,  $\beta_1$ ,  $\beta_2$ ,  $\beta_3$  and  $\beta_4$  = linear effect coefficients,  $\beta_{11}$ ,  $\beta_{22}$ ,  $\beta_{33}$ , and  $\beta_{44}$  = quadratic effect coefficients,  $\beta_{12}$ ,  $\beta_{13}$ ,  $\beta_{14}$ ,  $\beta_{23}$ ,  $\beta_{24}$  and  $\beta_{34}$  = interaction effect coefficients, X<sub>1</sub>, X<sub>2</sub>, X<sub>3</sub>, and X<sub>4</sub> = independent variables

**Table 5:** Design summary for optimization

Factor	Name	Units	Type	Low Actual	High Actual	Low Coded	High Coded	Mean	Std. Dev.
A	Pollution load	%	Numeric	20	100	-1	1	60	25.731
B	pH		Numeric	3	11	-1	1	7	2.573
C	H <sub>2</sub> O <sub>2</sub> load	Mole	Numeric	0.2	0.6	-1	1	0.4	0.129
D	Time	Mins	Numeric	10	90	-1	1	50	25.731

Response	Name	Units	Obs	Analysis	Minimum	Maximum	Mean	Std. Dev.	Ratio	Trans	Model
Y <sub>1</sub>	Colour removal	%	29	Polynomial	16.23	98.9	67.184	23.259	6.094	None	Quadratic
Y <sub>2</sub>	COD removal	%	29	Polynomial	7.05	86.07	47.479	22.919	12.209	None	Quadratic

For designing, analysis and response surface were studied using Design-expert (stat-Ease, trial version) software. All the graphs presented were generated using this software. After fitting of BBD data, the final equation was derived in terms of Colour removal and COD removal is given in equation 9 and 10.

$$\text{COD removal \%} = 67.65 - 19.72 A + 6.95 B + 13.98 C + 17.09 D - 3.78 AB + 0.90 AC + 0.62 AD + 8.61 BC + 7.80 BD + 4.12 CD - 11.71 A^2 - 19.78 B^2 - 4.75 C^2 - 12.51 D^2$$

$$\text{Colour removal \%} = 87.20 - 19.03 A + 2.94 B + 11.71 C + 22.52 D - 1.59 AB + 3.10 AC + 0.25 AD + 9.59 BC + 1.59 BD - 3.06 CD - 12.25 A^2 - 14.52 B^2 - 5.0 C^2 - 16.59 D^2$$

The model accuracy was checked by comparing the predicted and experimental oxidation efficiencies. Fig. 5.a

and 6.a shows the linear relationship between the predicted and experimental oxidation efficiencies. In this way, the residuals can be checked to determine how well the model satisfies the assumptions of ANOVA, and the internally studentized residuals can be used to measure the standard deviations separating the experimental and predicted values [24]. Fig. 5.b & 6.b shows the relationship between the normal probability (%) and the internally studentized residuals. The straight line means that there is no response transformation required and there was no apparent problem with normality. According to Table 6, responses for Colour and COD removal, the quadratic model was statistically significant (P <0.0001) [25]. Fig.7 and Fig.8 show the 3D surface plots for the colour removal and COD removal with respect to variable parameters.

**BBD and their experimental results**

**Table 6:** Sequential model sum of squares of responses

Source	For Colour Removal				For COD Removal			
	Sum of Squares	Mean Square	F Value	Prob > F	Sum of Squares	Mean Square	F Value	Prob > F
Mean	130898.89	130898.89			65373.31	65373.31		
Linear	12178.12	3044.53	20.82	< 0.0001	11095.45	2773.86	16.09	< 0.0001
2FI	464.08	77.35	0.46	0.8306	669.71	111.62	0.58	0.7421
Quadratic	3031.87	757.97	766.66	< 0.0001	3364.79	841.2	113.66	< 0.0001
Cubic	8.49	1.06	1.19	0.4286	90.23	11.28	5.06	0.0318
Residual	5.36	0.89			13.38	2.23		
Total	146586.79	5054.72			80606.87	2779.55		

**Table 7:** Model summary statistics for response

Source	Colour removal					COD removal				
	Std. Dev.	R <sup>2</sup>	Adjusted R <sup>2</sup>	Predicted R <sup>2</sup>	Press	Std. Dev.	R <sup>2</sup>	Adjusted R <sup>2</sup>	Predicted R <sup>2</sup>	Press
Linear	12.0930	0.7763	0.7390	0.7125	4509.7096	13.1309	0.7284	0.6831	0.6403	5478.843
2FI	13.0079	0.8059	0.6980	0.6424	5609.8179	13.8812	0.7723	0.6458	0.5442	6942.773
Quadratic	0.9943	0.9991	0.9982	0.9949	79.7259	2.7204	0.9932	0.9864	0.9608	596.7959
Cubic	0.9448	0.9997	0.9984	0.9508	771.1932	1.4934	0.9991	0.9959	0.8735	1926.955

**Table 8:** ANOVA for responses

Source	For Colour Removal				For COD Removal			
	Sum of Squares	Mean Square	F Value	p-value	Sum of Squares	Mean Square	F Value	p-value
Model	15674.0626	1119.5759	1132.4	< 0.0001	15129.9515	1080.7108	146.03	< 0.0001
A-Pollution load	4344.5491	4344.5491	4394.4	< 0.0001	4667.7241	4667.7241	630.71	< 0.0001
B-pH	103.8408	103.8408	105.03	< 0.0001	579.491	579.491	78.302	< 0.0001
C-H <sub>2</sub> O <sub>2</sub> load	1645.7234	1645.7234	1664.6	< 0.0001	2344.4461	2344.4461	316.79	< 0.0001
D-Time	6084.0033	6084.0033	6153.8	< 0.0001	3503.7919	3503.7919	473.44	< 0.0001
AB	10.0806	10.0806	10.196	0.0065	57.078	57.078	7.7125	0.0148
AC	38.502	38.502	38.944	< 0.0001	3.2041	3.2041	0.4329	0.5212
AD	0.245	0.245	0.2478	0.6263	1.5625	1.5625	0.2111	0.6529
BC	367.6806	367.6806	371.9	< 0.0001	296.5284	296.5284	40.067	< 0.0001
BD	10.1761	10.1761	10.293	0.0063	243.36	243.36	32.883	< 0.0001
CD	37.3932	37.3932	37.822	< 0.0001	67.98	67.98	9.1856	0.009
A <sup>2</sup>	973.9082	973.9082	985.07	< 0.0001	889.8968	889.8968	120.24	< 0.0001
B <sup>2</sup>	1367.941	1367.941	1383.6	< 0.0001	2537.9344	2537.9344	342.93	< 0.0001

C <sup>2</sup>	162.3785	162.3785	164.24	< 0.0001	146.223	146.223	19.758	0.0006	
D <sup>2</sup>	1785.7118	1785.7118	1806.2	< 0.0001	1014.3921	1014.3921	137.07	< 0.0001	
Residual	13.8413	0.9887			103.6104	7.4007			
Lack of Fit	13.8413	1.3841			103.6104	10.361			
Pure Error	0	0			0	0			
Cor Total	15687.9039				15233.5619				
				Std. Dev. = 0.99, C.V % = 1.48, Press = 79.73, R <sup>2</sup> = 0.9991, Adj R <sup>2</sup> = 0.9982 Pred R <sup>2</sup> = 0.9949, AP = 116.19					Std. Dev. = 2.72, C.V % = 5.73, Press = 596.80, R <sup>2</sup> = 0.9932, Adj R <sup>2</sup> = 0.9864, Pred R <sup>2</sup> = 0.9608, AP = 40.68

**Table: 9** Optimum operating conditions of the process variables for maximum colour removal and COD removal

Solution No.	Pollution load (%)	pH	H <sub>2</sub> O <sub>2</sub> load (mole)	Time (min)	Colour removal (%)	COD removal (%)	Desirability
2	64	8	0.6	81	98.77	86.11	1

The suitability of the optimized conditions for predicting the optimum response values was tested in the selected optimal conditions. Additional experiments using the predicted optimum conditions were carried out and the mean values were obtained from the experimental results were in agreement with the predicted values obtained from the model established (Table 9).

#### 4. Conclusion

The present study reveals that the treatment of efficiency of the UV/H<sub>2</sub>O<sub>2</sub> method for the degradation of the simulated effluent / real time effluent. Strongly influencing parameters such as initial H<sub>2</sub>O<sub>2</sub> concentration, pollution load and initial pH were studied to identify the optimum condition for the maximum treatment efficiency. A Box–Behnken design with the RSM was successfully applied to UV/H<sub>2</sub>O<sub>2</sub> treatment system on the treatability of simulated dye bath effluent. The treatment efficiency of the process increases with an increase in the concentration H<sub>2</sub>O<sub>2</sub> to the optimum value of 0.4 M, further increase in the concentration of H<sub>2</sub>O<sub>2</sub> will reduce the treatment efficiency. The degradation process follows first order kinetics with respect to the pollution load and the rate constant decreases with increasing pollution load. Variation in the initial pH also had a significant influence on the degradation efficiency. The maximum degradation efficiency was achieved in the neutral and slightly alkaline medium. Based on the statistical analysis (ANOVA), high coefficient of determining value (R<sup>2</sup>) 0.9991 for colour and 0.9932 for COD ensures a satisfactory fit of the second-order polynomial regression model with the experimental data. Additional experiments were carried out using the predicted optimum conditions and the values obtained were 98.01% for colour removal and 85.26% for COD removal in agreement with the predicted values obtained 98.77% for colour removal and 86.11% for COD removal.

#### 5. Acknowledgement

The authors greatly acknowledge the Department of Science & Technology (TSD), Government of India (Research Project No.DST/TSG/NTS/2012/67-G) for providing the financial support to carry out this research work and the experiments have been conducted at Centre for Environmental Research, Department of Chemistry, Kongu Engineering College, Perundurai, Erode – 638 052, TN, India.

#### References

- [1] A Hamza, M F Hamoda, Multiprocess. Treatment of Textile Wastewater. In Proceedings of the 35<sup>th</sup> Industrial Waste Conference, Purdue University, Lafayette, IN. (1980) 151.
- [2] U Pagga, D Brown. The degradation of dyestuffs in aerobic biodegradation tests, Chemosphere 15 (1986) 479–491.
- [3] HL Sheng, ML Chi. Treatment of textile waste effluents by ozonation and chemical coagulation, Wat Res. 27 (1993) 1743–1748.
- [4] KG Birchen, W Lem, KM Simms, BW Dussert. Combination of UV oxidation with other treatment technologies for remediation of contaminated water, J Adv Oxid Technol. 2 (1997) 345-441.
- [5] JR Boltan, SR Cater. Homogeneous photodegradation of pollutants in contaminated water: an Introduction. In: Helz GR, Zepp RG, Crosby DG, (Eds.) Aquatic and Surface Photochemistry, EEUU, Lewis, Boca Raton, FL. (1994) 467-490.
- [6] O Legrini, E Oliveros, AM Braun. Photochemical processes for Water treatment, Chem Rev. 93 (1993) 671-698.
- [7] HY Shu, CR Huang, MC Chang. Decolourization of mono-azo dyes in wastewater by advanced oxidation process: a case study of Acid Red 1 and Acid Yellow 23, Chemosphere 29 (1994) 2597–2607.
- [8] CG Namboodri, WK Walsh. Ultraviolet light/hydrogen peroxide system for decolourizing spent reactive dye bath waste water, American Dyestuff Reporter (1996) 15–25.
- [9] C Morrison, J Bandara, J Kiwi. Sunlight induced decolouration/degradation of non- biodegradable Orange II dye by advanced oxidation technologies is homogeneous and heterogeneous media, J Adv Oxid Technol. 1 (1996) 160– 169.
- [10] C Galindo, P Jacques, A Kalt. Total mineralization of an azo dye (Acid Orange 7) by UV/H<sub>2</sub>O<sub>2</sub> oxidation, J Adv Oxid Technol. 4 (1999) 400–407.
- [11] GM Colonna, T Caronna, B Marcandalli. Oxidative degradation of dyes by ultraviolet radiation in the presence of hydrogen peroxide, Dyes and Pigm. 41 (1999) 211–220.
- [12] P Manikandan, PN Palanisamy, R Baskar, P Sivakumar and P Sakthisharmila. Physico Chemical Analysis of Textile Industrial Effluents From Tirupur City, TN, India, Int J Adv Res Sci & Eng. 4 (2015) 93-104.

- [13] APHA. Standard methods for examination of water and wastewater, American public health association. WWA, Washington, D.C. (2005).
- [14] NH Ince, MI Stefan, JR Bolton. UV/H<sub>2</sub>O<sub>2</sub> degradation and toxicity reduction of textile azo dyes: remazol Black-B, a case study, *J Adv Oxid Technol.* 2 (1997) 442–448.
- [15] M Karkmaz, E Puzenat, C Guillard, JM Herrmann. Photocatalytic degradation of the elementary azo dye amaranth. Mineralization of the azo group to nitrogen, *Appl Catal B Environ.* 51 (2004) 183–194.
- [16] M Styliidi, DI Kondarides, XE Verykios. Visible light-Induced photocatalytic degradation of acid orange 7 in aqueous TiO<sub>2</sub> suspensions, *Appl Catal B.* 47 (2004) 189-201.
- [17] Z He, L Lin, S Song, M Xia, L Xu, H Ying et al. Mineralization of C.I. Reactive Blue 19 by ozonation combined with sonolysis: Performance optimization and degradation mechanism, *Sep Purif Technol.* 62 (2008) 376-381.
- [18] G Isil and H.I Nilsun. Degradation of Reactive Azo Dyes by UV/H<sub>2</sub>O<sub>2</sub>: Impact of Radical Scavengers, *J. Environ. Sci. Health.* 39 (2004) 1069–1081.
- [19] CH Liao, SF Kang, FA Wu. Hydroxyl radical scavenging role of chloride and bicarbonate ions in the H<sub>2</sub>O<sub>2</sub>/UV process, *Chemosphere.* 44 (2001) 1193-1200.
- [20] M Li, C Feng, Z Zhang, R Chen, Q Xue, C Gao et al. Optimization of process parameters for electrochemical nitrate removal using Box–Behnken design, *Electrochim Acta* (2010) 265–270.
- [21] P Tripathi, VC Srivastava, A Kumar. Optimization of an azo dye batch adsorption parameters using Box- Behnken design, *Desalination* 249 (2009) 1273–1279.
- [22] T Francesc, G Julia, Using central composite experimental design to optimize the degradation of real dye wastewater by Fenton and photo-Fenton reactions, *Dyes and Pigm.* 100 (2014) 184-189.
- [23] K Thirugnanasambandham, V Sivakumar, J Prakash Maran Response surface modeling and optimization of treatment of meat industry wastewater using electrochemical treatment method, *J Taiwan Inst Chem Eng.* 46 (2015) 160–167.
- [24] H.L. Liu, Y.R. Chiou, Optimal decolourization efficiency of Reactive Red 239 by UV/TiO<sub>2</sub> photocatalytic process coupled with response surface methodology, *Chem. Eng. J.* 112 (2005) 173 -179.
- [25] N Lavanyah and M Thanapalan, Degradation of Alizarin Yellow R using UV/H<sub>2</sub>O<sub>2</sub> Advanced Oxidation Process, *Environ Prog & Sustain Energy* 33 (2013) 482-489.